Downregulated expression of miRNA-149 promotes apoptosis in side population cells sorted from the TSU prostate cancer cell line

YATONG CHEN, JIAHUI ZHAO, YONG LUO, YONGXING WANG and YONGGUANG JIANG

Department of Urology, Beijing Anzhen Hospital, Capital Medical University,
Beijing Institute of Heart, Lung and Blood Vessel Diseases, Beijing 100029, P.R. China

Received February 22, 2016; Accepted March 30, 2016

DOI: 10.3892/or.2016.5047

Abstract. The objective of the present study was to identify prostate cancer stem cells and determine the effects of modulating specific miRNAs on prostate CSC proliferation and apoptosis. We applied flow cytometry sorting of side population cells to cultures of prostate cancer cell lines (TSU, DU145, PC-3 and LNCaP). The proportion of SP cells in the TSU line was 1.60±0.40% (mean ± SD), while that of the DU145, PC-3 and LNCaP lines was 0.60±0.05, 0.80±0.05 and 0.60±0.20%, respectively. Because the proportion of SP cells derived from TSU cells is greater, these cells were selected to sort side population cells and non-side population cells. The stem-like properties of SP cells had been identified by *in vivo* and *in vitro* experiments, and the related study was published. RNA was extracted from the SP cells and non-SP cells and analyzed using miRNA microarray technology. Fifty-three miRNAs with significant differences in their expression were detected in total. Furthermore, 20 of these miRNAs were validated by qPCR. We found that hsa-miR-149 expression in SP cells and non-SP cells was significantly different; hsa-miR-149 was significantly upregulated in SP cells. By constructing a vector for lentiviral infection, we found that the downregulation of hsa-miR-149 leads to a reduction in proliferation, an increase in apoptosis, and a significant reduction in the colony formation potential, thus, inhibiting tumor growth *in vivo* of SP cells from the TSU cell line. The present study will provide new avenues toward understanding the function of prostate cancer stem cells (PCSCs) in tumorigenicity and metastasis.

Introduction

Tumor conquest remains a difficult problem for the medical community. Malignant tumors severely threaten human health and life. The key to tumor treatment is finding a specific target and effectively inhibiting the source of the tumor. Finding cancer stem cells makes targeted tumor tissue killing, tumor cure and tumor recurrence and metastasis prevention possible. Through profound research on the biological characteristics of cancer stem cells (CSCs) and their mechanisms, a specific CSC-targeted treatment represents a new method to cure cancer. The research on CSCs is prospective but difficult. The proportion of CSCs in tumor tissue is small, and most of them are in a stationary phase and are only active in a specific tumor micro-environment in which they directionally differentiate into a certain type of cancer cell. Chemotherapy drugs only work on active cells that are in the multiplication and division phases, which allows the CSCs in a stationary phase to evade the effects of the drugs. In time, the latent CSCs will multiply and differentiate into ordinary cancer cells, which becomes the clinical origin of cancer recurrence and metastasis after chemotherapy (1). Therefore, a systematic understanding of the biological behavior, gene phenotype, signal transduction pathways, and control mechanisms for the multiplication and division of CSCs will help improve the clinical rate of curing cancer.

For decades, scientists have tried to use different methods to separate stem cells and have widely shown that CSCs exist in different types of cancer tissues (2-4). However, because some cancer tissues lack specific stem cell surface markers, the separation and isolation of stem cells is difficult and becomes a barrier for functional studies. The development of side population cell research provides a new direction for CSC research (5). It has been found that side population cells exist not only in the bone marrow hematopoietic system but also widely in other normal tissues such as the nervous system, liver, spleen and even tumor tissues (6,7). Like stem cells, side population cells have not only a potential for self-renewal and multilineage differentiation but also special phenotypic markers and biological characteristics. The rapid Hoechst dye rejection feature of these cells provides a more convenient method for stem cell research and can be used as a separation method for CSCs that lack known surface markers. Therefore, a side population cell separation method would lay a solid foundation for more comprehensive research on CSCs.

In recent years, there has been a breakthrough in microRNA (miRNA) research and a large number of miRNA molecules have been identified. It has been shown that miRNAs play

Correspondence to: Professor Yongguang Jiang, Department of Urology, Beijing Anzhen Hospital, Capital Medical University, Beijing Institute of Heart, Lung and Blood Vessel Diseases, Beijing 100029, P.R. China
E-mail: yongguangjiang@126.com

Key words: cancer stem cells, side population cells, prostate cancer, microRNA, apoptosis

key regulatory roles in the maintenance of cell surface phenotypes and in the process of differentiation: i) miRNAs are evolutionarily highly conserved molecules with clear cell and tissue specificity. Approximately 1/3 of human genes can be regulated by miRNAs. Therefore, miRNAs have a large impact on the balance of intracellular signaling networks and in coordinating multi-gene regulation (8-10). ii) miRNAs exhibit clear differences in different cell types or even in different differentiation phases of the same cell type and regulate cell differentiation. It has been shown that miR-155 is involved in regulating T cell differentiation (11). miR-221 and miR-222 are involved in regulating red blood cell differentiation (12). miR-124 is involved in regulating the differentiation of the central nervous system (13). miRNA-128 is enriched in brain and may have biological functions and therapeutic potential (14). miR-191 has been recently reported to be abnormally expressed in several cancers and various other diseases such as type-2 diabetes, Crohn's, pulmonary hypertension and Alzheimer's (15). iii) miRNAs are key molecules in the maintenance of cell proliferation, phenotype and differentiation processes, and also regulate tumorigenesis and metastasis of cancer cells or cancer stem cells. The miR-92a family and miR-210 have a close relationship with malignant tumors both in their development and metastasis (16,17). miR-101 targets EZH2, MCL-1 and FOS to suppress proliferation, invasion and the stem cell-like phenotype of aggressive endometrial cancer cells (18). miR-146a enhances *helicobacter pylori*-induced cell apoptosis in human gastric cancer epithelial cells (19), and miR-338 and miR-30b inhibit the growth, invasion and metastasis of gastric cancer (20,21). Overexpression of miR-203 in esophageal cancer cells markedly increases cell apoptosis and inhibits cell proliferation, migration and invasion as well as tumor growth (22). Knockdown of miR-214 promotes apoptosis and inhibits cell proliferation in nasopharyngeal carcinoma (23). miR-130b and miR-27a suppress the migration and invasion of colorectal cancer cells (24,25). miR-545 and miR-203 suppress cell proliferation and promote apoptosis in lung cancer cells by targeting cyclin D1 and CDK4 or by targeting SRC in lung cancer cells (26,27). The lack of Dicer1 (the key enzyme in miRNA production) can lead to a decrease in mouse embryonic stem cells and the death of mouse embryos (28). miRNA molecules can promote the conversion from the G1 phase to the S phase in stem cells, thereby promoting their proliferation (29). In neural glioma stem cells, overexpression of miR-124 and miR-137 can lead to the loss of self-renewal and tumorigenicity (30), and the anti-apoptotic miRNAs miR-582-5p and miR-363 promote human glioblastoma stem cell survival via direct inhibition of caspase-3 and caspase-9 (31). In melanoma, miR-143 targets syndecan-1 to repress cell growth (32). As miRNA molecules play an important role in regulating stem cell differentiation, the identification of which miRNA molecules play the decisive roles in different cell types has become an impending problem of immediate concern.

The incidence of prostate cancer has remained high worldwide, becoming a serious threat to human health, and is the second most common cancer-related cause of death in males (33). In the United States, the incidence of prostate cancer is the highest among male malignancies, and its mortality rate is second only to lung cancer. Approximately 230,000 people are diagnosed with prostate cancer every year and 30,000 die from it. The introduction of the prostate cancer stem cell theory has provided a new thinking regarding prostate cancer treatment. Early experiments in the literature have reported that specific stem cell surface markers have not been found for common prostate cancer cell lines such as LNCaP and TSU, which makes it difficult to isolate prostate cancer stem cells. Therefore, the research on prostate cancer stem cells is lagging in comparison to other cancers. The objective of the present study was to identify prostate cancer stem cells and determine the effects of modulating specific miRNAs on prostate CSC proliferation and apoptosis. We have used a side population cell separation method to separate SP cells and the stem-like properties of SP cells have been identified by *in vivo* and *in vitro* experiments, and a related study was published (34). This established a prostate cancer stem cell separation and identification technology platform, and further applied biochip and real-time quantitative PCR technology to separate prostate cancer stem cell-specific miRNAs. By interfering with the expression of miRNAs in CSCs, we can study the changes in the biological functions of prostate cancer stems cells. These results may promote the research and development of miRNA-targeted drugs and create a new approach for the clinical treatment of prostate cancer.

Materials and methods

Cell culture. The human prostate cancer cell lines DU145, PC-3 and LNCaP were purchased from the American Type Culture Collection (ATCC; Manassas, VA, USA) and the TSU cell line was provided by the Cancer Institute, Chinese Academy Of Medical Sciences (Beijing, China). All cell lines were conserved in our own laboratory. Cells were cultured in media (TSU, DU145 and PC-3 used DMEM-F12; LNCaP used RPMI-1640) (Gibco, Carlsbad, CA, USA) supplemented with 10% fetal bovine serum (FBS; Gibco), 100 units/ml penicillin, and 0.1 mg/ml streptomycin at 37˚C in a humidified 5% CO_2 incubator. Cells were cultured for two or three passages and then used for an experiment in the exponential phase of growth.

Flow cytometry. The generally accepted method for sorting side population cells was utilized to identify and isolate SP fractions. TSU, DU145, PC-3 and LNCaP cells were dissociated from culture flasks with trypsin-EDTA (Beijing Neuronbc Laboratories, Co., Ltd., Beijing, China) and pelleted by centrifugation. The cells were resuspended at $1x10^6$ cells/ml in pre-warmed culture media (TSU, DU145 and PC-3 used DMEM-F12; LNCaP used RPMI-1640) (Gibco) with 2% bovine serum albumin (BSA; Gibco) and 10 mmol/l N-(2-hydroxyethyl)piperazine-N'-(2-ethanesulfonic acid) (HEPES). Hoechst 33342 dye (Sigma-Aldrich, St. Louis, MO, USA) was added to a final concentration of 5 μg/ml in the presence or absence of 50 μM verapamil (Sigma-Aldrich), and cells were then incubated at 37˚C for 90 min. After incubation, the cells were washed with ice-cold 1X PBS, pH 7.4 three times. Prior to analysis or sorting, propidium iodide (2 μg/ml; Sigma-Aldrich) was added immediately to discriminate dead cells and the cells were filtered through 80 μm mesh (Becton-Dickinson Co., Franklin Lakes, NJ, USA) to obtain a single cell suspension. Samples were then analyzed using a BD LSR II 4-laser

Table I. The RNA area, RNA concentration, and rRNA ratio [28s/18s] of the SP and non-SP groups isolated from TSU.

	Ladder	Non-SP	SP
RNA area	599.6	153.6	155.2
RNA concentration (pg/μl)	1000	256	259
rRNA ratio [28s/18s]		1.4	1.2

flow cytometer (BD Biosciences, San Jose, CA, USA). The Hoechst 33342 dye was excited at 355 nm and its fluorescence was dual-wavelength analyzed with the emission for Hoechst blue at 445 nm and Hoechst red at 650 nm.

miRNA microarray assay. The different expression levels of miRNAs between the SP cells and non-SP cells isolated from the TSU cell line were detected using a miRNA microarray. The results of the sample quality control analysis are shown in Fig. 1A; the RNA concentration of the SP group was 259 pg/μl, with an rRNA ratio [28s:18s] of 1.2; the RNA concentration of the non-SP group was 256 pg/μl, with an rRNA ratio [28s:18s] of 1.4 (Table I). All of these measurements met the standard quality conditions for the microarray analysis. The microarray assay was performed using a service provider (LC Sciences, Houston, TX, USA). A total of 1208 types of miRNAs were detected. The assay started from 2 to 5 μg of a total RNA sample that was size fractionated using a YM-100 Microcon centrifugal filter (from Millipore) and the small RNAs (<300 nt) isolated were 3'-extended with a poly(A) tail using poly(A) polymerase. An oligonucleotide tag was then ligated to the poly(A) tail for later fluorescent dye staining; two different tags were used for the two RNA samples in dual-sample experiments. Hybridization was performed overnight on a μParaflo™ microfluidic chip using a micro-circulation pump (Atactic Technologies, Inc., Houston, TX, USA). On the microfluidic chip, each detection probe consisted of a chemically modified nucleotide coding segment complementary to the target miRNAs (from miRBase, http://miRNA.sanger.ac.uk/sequences/) or other RNA (control or customer defined sequences) and a spacer segment of polyethylene glycol to extend the coding segment away from the substrate. The detection probes were made by *in situ* synthesis using PGR (photogenerated reagent) chemistry. The hybridization melting temperatures were balanced by chemical modifications of the detection probes. The hybridization used 100 μl 6X SSPE buffer (0.90 M NaCl, 60 mM Na_2HPO_4, 6 mM EDTA, pH 6.8) containing 25% formamide at 34˚C. After hybridization, signal detection was based on fluorescent labeling using tag-specific Cy3 and Cy5 dyes. Hybridization images were collected using a laser scanner (GenePix 4000B; Molecular Devices, Sunnyvale, CA, USA) and digitized using Array-Pro image analysis software (Media Cybernetics, Rockville, MD, USA). Data were analyzed by first subtracting the background and then normalizing the signals using a LOWESS filter (Locally weighted regression). For two-color experiments, the ratio of the two sets of detected signals (log_2 transformed, balanced) and the P-values of the t-test were calculated; differentially detected signals were those with P<0.01.

RNA extraction and real-time PCR. qRT-PCR was performed to determine the different expression levels of miRNAs between the SP and non-SP of TSU cells. Total RNA was extracted from the corresponding cells using TRIzol reagent (Invitrogen Life Technologies, Waltham, MA, USA). In the reverse transcription (13) step, complementary DNA (cDNA) was reverse transcribed from the total RNA samples using specific miRNA primers and a TaqMan Reverse Transcription kit (Applied Biosystems, Carlsbad, CA, USA). In the real-time PCR step, PCR products were amplified from the cDNA samples using the TaqMan miRNA Assay together with the TaqMan Universal PCR Master Mix (Applied Biosystems) (Fig. 1B). An ABI PRISM 7000 Sequence detection system (Applied Biosystems) was the main experimental instrument. Using the comparative CT method, we used TaqMan endogenous controls to normalize the expression levels of target genes by correcting for differences in the amount of cDNA loaded into the PCR reactions. Each sample was run in triplicate.

Oligonucleotide construction. The hsa-miR-149-3p-inhibition oligonucleotide was chemosynthesized (Shanghai GenePhama Co., Ltd., Shanghai, China). The sequence of the oligonucleotides used in the present study was for the target sequence documented in the miRNA Registry database: 5'-GCACAGC CCCCGTCCCTCCCT-3'; synthesized hsa-miR-149-3p-inhibition: 5'-AATTCAAAAAAGGGAGGGACGGGGGCTGT GC-3' and 5'-CCGGGCACAGCCCCCGTCCCTCCCTTTTT TG-3'.

The results of the vector construction and lentiviral infection. To study the impact of the miRNA-149 downregulation on the functional alteration of TSU-derived SP cells, we designed and constructed a miRNA-149-inhibition lentiviral vector. Fig. 2A shows the plasmid vector containing green fluorescent protein (GFP). Fig. 2B demonstrates the synthesis of the desired gene fragment for miRNA-149-inhibition. Synthetic oligonucleotides were as follows: hsa-miR-149: 5'-UCUGGCU CCGUGUCUUCACUCCC-3'; hsa-miR-149-3p-inhibition-a: 5'-AATTCAAAAAAGGGAGGGACGGGGGCTGT GC-3'; hsa-miR-149-3p-inhibition-b: 5'-CCGGGCACAGCC CCCGTCCCTCCCTTTTTTg-3'.

The desired plasmid was constructed via restriction enzyme digestion, ligation and transformation. Fig. 2C depicts the sequencing results of the constructed plasmid.

The sequencing primer: 5'-GGAAAGAATAGTAGACAT AATAGC-3'. The constructed plasmid sequence: 5'-CAAAA-CAAATTACAAAAATTCAAAATTTTCGGGTTTATTAC AGGGACAGCAGAGATCCAGTTTGGTTAGTACCGGGC CCGCTCTAGACTCGAGATATTTGCATGTCGCTATGGT TCTGGGAAATCACCATAAACGTGAAATGTCTTTGG ATTTGGGAATCTTATAAGTTCTGTATGAGACCACTCAC CGGGCACAGCCCCCGTCCCTCCCTTTTTTGAATTCGG ATCCATTAGGCGGCCGCGTGGATAACCGTATTACCGC CATGCATTAGTTATTAATAGTAATCAATTACGGGGTA TTAGTTCATGCCCATATATGGAGTTCCGCGTTACATAA CTTACGGTAAATGGCCCGCCTGGCTGACCGCCCAAC GACCCCCGCCCATTGACGTCAATAATGACGTATGTT CCCATAGTAACGCCAATAGGGACTTTCCATTGACGTC AATGGGTGGAGTATTTACGGTAAACTGCCCACTTGG

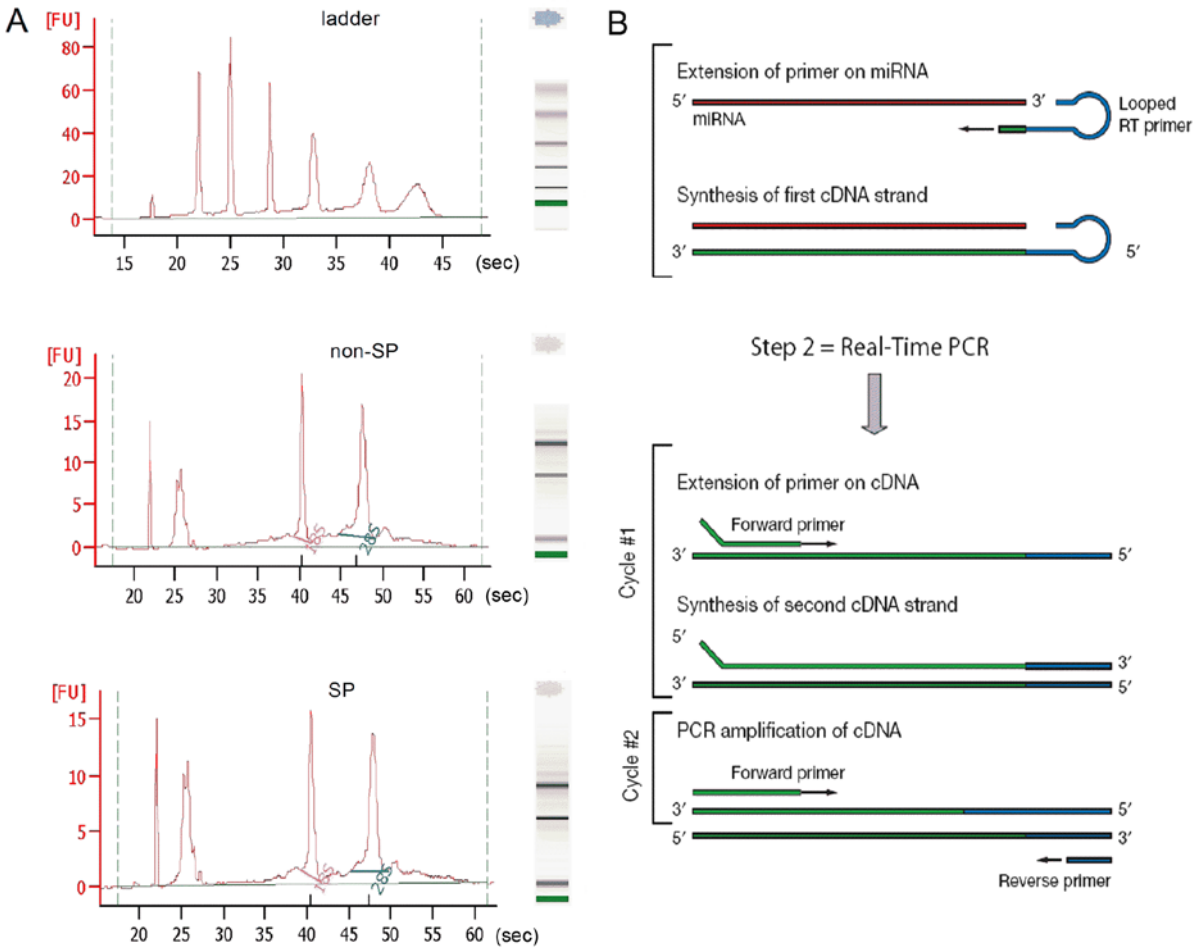

Figure 1. Results of the sample quality control analysis and process of TaqMan microRNA qRT-PCR. (A) Quality control analysis of the RNA concentration from the SP and non-SP groups isolated from TSU; (B) structure of the TaqMan probe and the technical process of qRT-PCR.

CAGTACATCAAGTGTATCATATGCCAAGTACGCCCCCT ATTGACGTCAATGACGGTAAATGGCCCGCCTGGCATT ATGCCCAGTACATGACCTTATGGGACTTTCCTACTTGG CAGTACATCTACGTATTAGTCATCGCTATTACCATGGT GATGCGGTTTTGGCAGTACATCAATGGGCGTGGATAG CGGTTTGACTCACGGGGATTTCCAAGTCTCCACCCC ATTGACGTCAATGGGAGTTTGTTTTGGCACCAAAATC AACGGGACTTTCCAAAATGTCGTAACAACTCCGCCCC ATTGACGCAAATGGGCGGTAGGCGTGTACGGTGGGA GGTCTATATAAGCAGAGCTGGTTTAGTGAACCGTCAG ATCCGCTAGCGCTACCGGACGCCACCATGGTGAGCA AGGGCGAGGAGCTGTTCACCGGGGTGGTGCCCATCCT GTCGAGCTGGACGGCGACGTAAACGCCACAAGTTCA GCGTGTCCGGCGAGGGCGAGGGCGATGCCACCTACG GCAAGCTGACCCTGAAGG-3'.

The constructed plasmid containing the gene fragment miRNA-149-inhibition was packaged into and produced as a lentivirus, which was used to infect cells. The viral titer was 2.5E +9. Fig. 2D shows the 4 different conditions for the miRNA-149-inhibition lentiviral infection of TSU-derived SP cells. The optimal infection condition, with an infection efficiency of up to 80%, was Eni.S; MOI 20-50.

Vector constructs and lentivirus production. The chemosynthesized hsa-miR-149-3p-inhibition oligonucleotide and the vector GV159 (Shanghai Genechem, Co., Ltd., Shanghai, China) were digested with the restriction enzymes *Age*I and *Eco*RI, respectively, and then connected with ligase. After transforming into DH5α, the pGCsil-GFP-hsa-miR-149-3p-inhibition clone was verified by sequencing. The sequencing primer was constructed as follows: 5'-GGAAAGAATA GTAGACATAATAGC-3'. The newly constructed clone pGCsil-GFP-hsa-miR-149-3p-inhibition and the negative control pGCsil-GFP-NC were amplified. Virus packaging was performed in HEK 293T cells after the co-transfection of 20 mg pGCsil-GFP-hsa-miR-149-3p-inhibition vector or pGCsil-GFP-NC vector with 15 mg of the packaging plasmid pHelper 1.0 vector and 10 mg of the envelope plasmid pHelper 2.0 vector using Lipofectamine 2000 (Invitrogen). Viruses were harvested 48 h after transfection, named pGCsil-GFP-hsa-miR-149-3p-inhibition-LV and pGCsil-GFP-NC-LV, respectively, and the viral titers were determined.

Cell infection. SP cells isolated from the TSU cell line were cultured to 30-50% confluency for the stable infection of cells after being seeded into 96-well plates and were infected in 4 different infection conditions: normal complete media; normal complete media with 5 μg/ml polybrene; ENi.S media (Shanghai GeneChem); and ENi.S media with 5 μg/ml polybrene. In each infection condition, three different gradient MOI were oper-

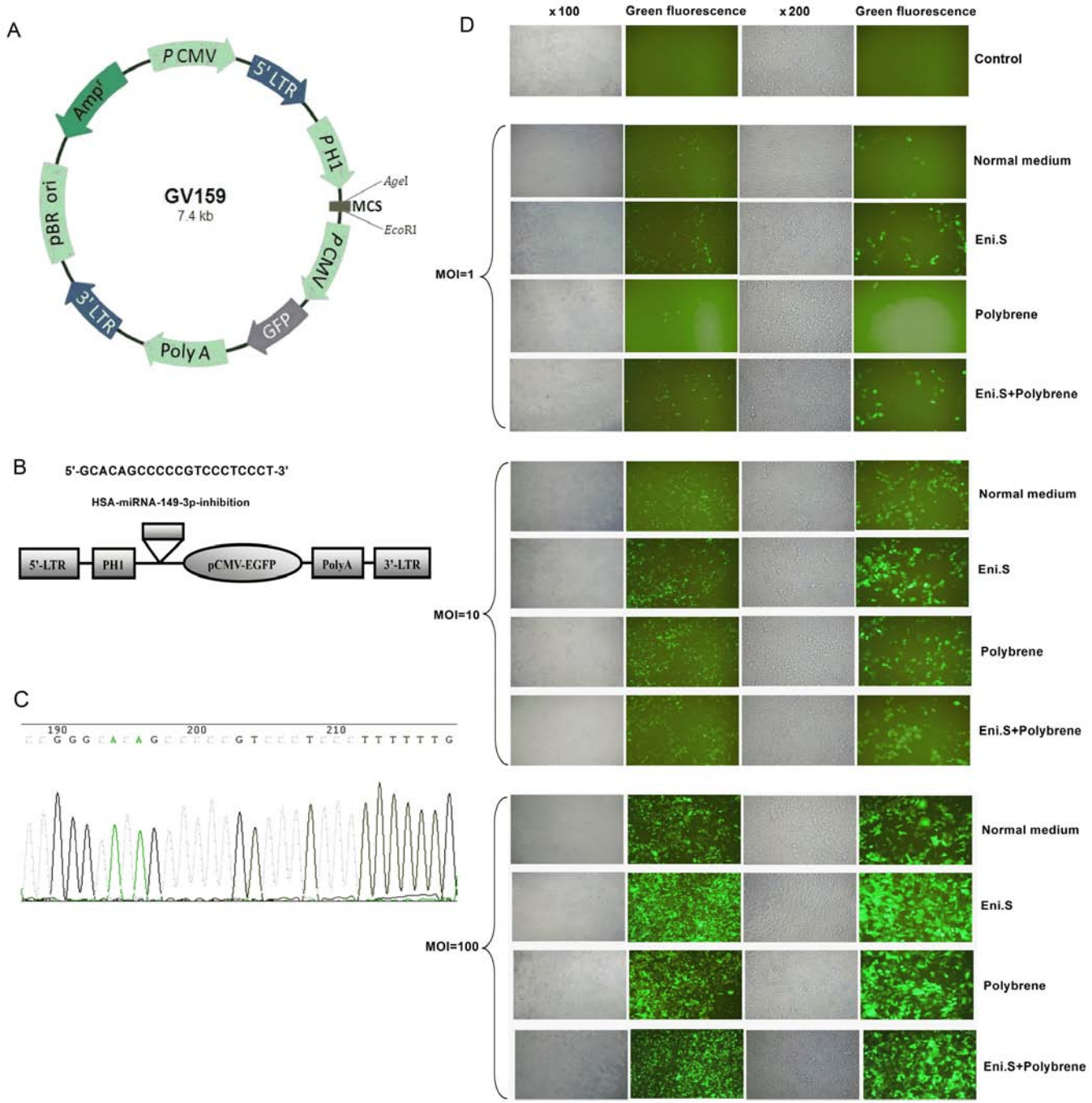

Figure 2. Vector construction and lentiviral infection. (A) The plasmid vector containing green fluorescent protein (GFP), (B) the synthesis of the desired gene fragment miRNA-149-inhibition, (C) the sequencing results of the constructed plasmid which contains the gene fragment miRNA-149-inhibition, and (D) 4 different infection conditions for miRNA-149-inhibition lentiviral infection of TSU-derived SP cells.

ated, including MOI=1; MOI=10 and MOI=100. After 72-h infection, the cells were harvested for further experimentation.

Cell proliferation assays. To compare a change in cell proliferation potential when the expression level of miRNA-149 was downregulated in TSU-derived SP cells, the MTT method was utilized to detect the ability of cell proliferation. Three different groups were designed to fulfill this experiment, including the SP cells derived from TSU that were infected with pGCsil-GFP-hsa-miR-149-3p-inhibition-LV (miRNA down group), the SP cells derived from TSU that were infected with pGCsil-GFP-NC-LV (negative control), and uninfected SP cells derived from TSU (control). Each group of cells was cultured in the logarithmic growth phase, counted and diluted to 20,000 cells/ml using complete media. One hundred microliters of cells (2,000 total cells) were added to each well (96-well culture plates) and incubated overnight. Each group was split into three duplicate wells. After 24 h of culture, 10 μl of 5 mg/ml MTT was added to each well. The cells were incubated for 4 h at 37˚C; then, the media was carefully removed and replaced with 100 μl DMSO to terminate the reaction. All of the experimental steps were performed aseptically. Cells were agitated on an orbital shaker for 10 min and the absorbance was read at 490 nm with the microplate reader (BioTek

Elx800; BioTek Instruments, Inc., Winooski, VT, USA). The same method was used for additional 96-well culture plates to detect the absorbance at 490 nm after 48, 72, 96 and 120 h.

Colony formation assays. To detect the impact of miRNA-149 downregulation on the colony formation potential of TSU-derived SP cells, colony formation assays were utilized. The miRNA down group consisted of the SP cells derived from TSU that were infected with pGCsil-GFP-hsa-miR-149-3p-inhibition-LV; the negative control group was the SP cells derived from TSU that were infected with pGCsil-GFP-NC-LV; and the control group was the SP cells derived from TSU. Each group of cells was cultured in the logarithmic growth phase, digested and counted. A total of 800 cells were added into each well (6-well culture plates) and incubated. Each group contained three duplicate wells. The media was changed and the cells were observed every 3 days. When the number of cells in most colonies was >50 (~14 days), the cell clones were photographed using a fluorescence microscope (Olympus MicroPublishe 3.3 RTV; Olympus, Tokyo, Japan) and then the culture was terminated. The cells were washed once with PBS, then 1 ml of paraformaldehyde was added to each well and fixed for 45 min and washed once with PBS. A 500 μl aliquot of Giemsa dye (ECM550; Chemicon International, Inc., Temecula, CA, USA) was added to each well and stained for 20 min. The cells were washed several times with ddH_2O until the background was clear and dried. The entire 6-well culture plates were photographed with a digital camera and images of the monoclonals were acquired using a microscope.

Cell apoptosis assays. Cells from the three groups were cultured in the same conditions, and the same number of cells was collected from the three groups and performed in triplicate. The entire experimental process was carried out in accordance with the instructions for the Apoptosis Detection kit (eBioscience 88-8007; eBioscience, Inc., San Diego, CA, USA). All the groups were analyzed using flow cytometry (FACSCalibur; BD Biosciences) within 4 h.

Cell cycle assays. Cells from the three groups were cultured to 80% confluency. Then, $2x10^6$ cells from each group (in triplicate) were collected and pelleted by spinning at 1,000 rpm, at 4˚C for 5 min. The cell pellets were resuspended in 1 ml of cold PBS and fixed by adding 4 ml of -20˚C absolute ethanol. The cells were stored at -20˚C in this fixation buffer until further analysis. The fixed cells were centrifuged (as above) and resuspended in 1 ml of PBS. A 100 μl aliquot of 200 μg/ml DNase-free, RNaseA was added, and the suspension was incubated at 37˚C for 30 min. Then, 100 μl of 1 mg/ml propidium iodide (light sensitive) was added and incubated at room temperature for 10 min. The samples were transferred to 12x75 Falcon tubes and read on a BD FACSCalibur (BD Biosciences).

In vivo tumor formation model. To determine whether there are differences in the tumorigenic potential and tumor growth when miRNA-149 was downregulated in TSU-derived SP cells, male nude mice (nu/nu genotype) 5 weeks of age were purchased from Vital River Laboratory Animal Technology Co., Ltd., Beijing, China. All animals were housed in an air-conditioned room under specific pathogen-free (SPF) conditions at 22±2˚C and 55±5% humidity with a 12-h light/dark cycle. Food and tap water were available at all times. All operations were carried out under the approval of the Capital Medical University Animal Experiments and Experimental Animals Management Committee, China. Experimental procedures conformed to animal welfare and minimized pain and suffering and the use of fewer animals. Twelve mice were divided into 3 groups. Each group of cells was suspended in serum-free DMEM-F12 media. Then $3x10^5$ cells in a volume of 100 μl were injected subcutaneously into the flanks of immune-compromised nude mice for each of the three cell groups to evaluate their tumorigenic activity and tumor growth. The mice were monitored daily for the appearance of subcutaneous tumors from the second day after the injection. For all mice, the tumor size was measured every 5 days from the 2nd day after the injection. After 37 days, the mice were sacrificed by cervical dislocation under chloral hydrate anesthesia, the tumor tissues were collected and the tumor volume was calculated using the following formula: 0.52 x length x $width^2$. Immunohistochemistry images for H&E staining, Ki-67 staining and Bax staining in the three groups.

Immunohistochemistry. The tumors were harvested at 37 days, and fixed in 10% formaldehyde solution, then embedded in paraffin. Sections (5 mm thick) that had been deparaffinized and rehydrated were stained with hematoxylin and eosin. Proliferating tumor cells were stained by Ki-67. Apoptotic tumor cells were stained by Bax. Images were collected by using microscope with x100 magnification.

Statistical analysis. A Student's t-test (two-tailed) one-way ANOVA and Mann-Whitney test were employed to analyze the data using the SPSS 12.0 software (SPSS, Inc., Chicago, IL, USA). A P-value of 0.05 was defined as being statistically significant, $P<0.05$; $P<0.01$.

Results

The existence of a SP in prostate cancer cells. The existence of an SP fraction in prostate cancer cells was confirmed by staining with Hoechst 33342 dye to generate a Hoechst blue-red profile. A small fraction of low-fluorescing cells in the lower-left region of each profile was gated as the SP. The appearance of this fraction was blocked by verapamil, an ABC transporter inhibitor. TSU cells contained a distinct fraction as an SP. In contrast, DU145, PC-3 and LNCaP cells had a much smaller SP fraction (Fig. 3). The SP proportion of TSU cells was calculated to be 1.60±0.40% (mean ± SD), while that of DU145, PC-3 and LNCaP cells was 0.60±0.05, 0.80±0.05 and 0.60±0.20%, respectively (Table II). Once identified, the cells within the SP gate were sorted into a flow tube by FACS.

Identification of stem-like properties in side population cells sorted from the TSU prostate cancer cell line. The stem-like properties of SP cells from TSU were identified by *in vivo* and *in vitro* experiments, and a related study was published (34).

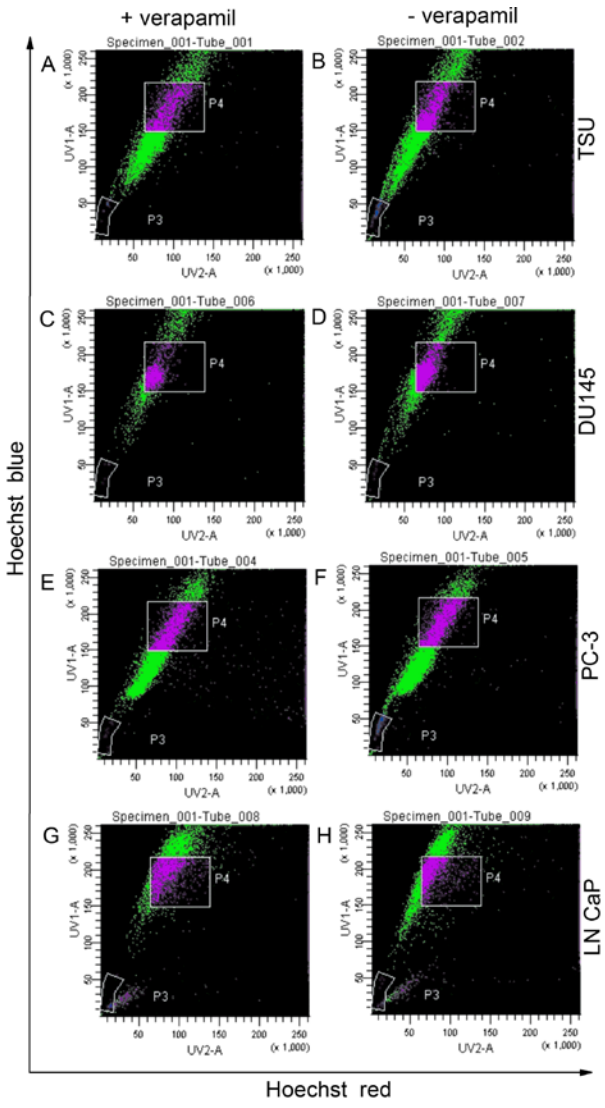

Figure 3. Flow cytometric side population analysis. (A, C, E and G) The side population (SP) cells in TSU, DU145, PC-3 and LNCaP disappeared (0.0%) when the cells were treated with 50 μM verapamil. (B, D, F and H) Representative SP were identified in the P3 gate of the flow cytometry profile after the cells were stained with Hoechst 33342.

Expression profiling of miRNAs between TSU-derived SP cells and non-SP cells. Dual-channel miRNA biochips from LC Sciences were used to analyze the differences in the miRNA expression profiles between the SP cells and non-SP cells isolated from the TSU cell line. Fig. 4A presents an image of the microarray experiments and demonstrates the results of the comparative analysis of the miRNA expression profiling of the two groups. In total, 53 significantly differentially expressed miRNAs were listed (Table III), and only a subset of the results were screened (Fig. 4B). Twenty miRNAs are significantly upregulated in SP, in which the most significantly upregulated miRNAs are hsa-miR-1246, hsa-miR-1908, hsa-miR-149. Thirty-three miRNAs are significantly downregulated in SP, in which the most significantly downregulated miRNAs are hsa-miR-451, hsa-miR-486-5p and hsa-miR-22. The greater the absolute value of the $\log_2$ (hybridization signal of the SP group/hybridization signal of the non-SP group), the greater the difference between the two groups, and the easier it is to distinguish the cancer stem cell-specific miRNAs. In addition to considering the multiple relationships of the signal strengths, the arithmetic difference of the signal intensity is also important to assess the difference between the two groups. The greater the arithmetic difference, the greater the significance.

Table II. The mean SP proportion of TSU, DU145, PC-3 and LNCaP (P<0.01).

Cells	SP proportion (mean ± SEM)
TSU	1.60±0.40%
DU145	0.60±0.05%
PC-3	0.80±0.05%
LNCaP	0.60±0.20%

qRT-PCR validation results. Given the high accuracy and specificity of the TaqMan probe method, and due to the limitations of the probes themselves, majority of the miRNAs were selected for further verification. Among the 53 significantly differentially expressed miRNAs identified in the biochips experiments, the top ten most significantly differentially expressed ones in downregulated and upregulated miRNAs were further validated using qRT-PCR experiments. The results are shown in Fig. 4C, the P-values of hsa-miR-451, hsa-miR-1246, hsa-miR-486-5p, hsa-miR-1908, hsa-miR-149, hsa-miR-1275, hsa-miR-3185, hsa-miR-22, hsa-miR-3613-3p, hsa-miR-3621, hsa-miR-3141, hsa-miR-3195, hsa-miR-99a, hsa-miR-19b, hsa-miR-222, hsa-miR-663, hsa-miR-762, hsa-miR-31, hsa-miR-100, and hsa-miR-29a for the comparison between the SP and non-SP groups were 5.96E-02, 2.68E-01, 6.48E-02, 3.54E-02, 6.04E-03, 6.68E-01, 4.25E-02, 8.54E-03, 5.25E-02, 6.36E-01, 7.35E-01, 5.28E-01, 6.26E-02, 5.16E-01, 2.48E-01, 2.58E-01, 6.88E-03, 8.24E-02, 4.42 E-01 and 4.22E-01, while the fold changes were -2.89, 2.66, -2.76, 2.85, 3.09, 1.98, 2.48, -2.53, -2.66, 2.49, 1.94, 2.66, -1.84, -2.21, -1.22, 1.42, 1.53, -1.64, -1.10 and -1.14, respectively. In accordance with the standard that the difference is significant and meaningful when the fold change is >3.0 and P-values <0.01, hsa-miR-149 was identified as being significantly upregulated in TSU-derived SP cells.

The downregulation of miRNA-149 leads to a reduction in proliferation and an increase in apoptosis in TSU-derived SP cells. The experimental design was grouped as follows: TSU-derived SP cells that were not infected (control); TSU-derived SP cells that were infected with the lentiviral vector alone (negative control); and TSU-derived SP cells that were infected with the constructed lentivirus containing the miRNA-149-inhibition fragment (micro down). Fig. 5A shows representative images of the three groups, which were treated under the same conditions, including media, culture time and MOI (MOI=20). Fig. 5B shows the results of the cell cycle assay. The number of cells in the S phase was significantly greater in the micro down group than the other two groups; for the G1 phase, the number of cells in the micro down group was significantly less than the control group, and slightly less

Table III. Significant differentially expressed microRNAs in SP compared with non-SP (P<0.01).

	microRNAs[a]	Non-SP signal[b]	SP signal[c]	$\log_2$ (SP signal/non-SP signal)[d]	P-value[e]
20 miRNAs upregulated					
	hsa-miR-1246	21.99	221.26	3.60	1.46E-04
	hsa-miR-1908	49.85	242.91	2.28	1.08E-05
	hsa-miR-149	621.39	2,228.20	1.87	2.22E-16
	hsa-miR-1275	330.53	1,141.12	1.76	1.32E-13
	hsa-miR-3185	542.63	1,866.65	1.76	8.88E-16
	hsa-miR-3621	367.35	1,262.98	1.69	2.51E-10
	hsa-miR-3141	788.83	2,713.54	1.68	3.33E-16
	hsa-miR-3195	353.59	1,030.08	1.58	6.12E-11
	hsa-miR-663	2,649.39	7,227.58	1.45	1.74E-08
	hsa-miR-762	3,379.81	7,789.94	1.20	7.70E-04
	hsa-miR-3178	2,989.62	6,215.48	1.11	1.65E-14
	hsa-miR-940	96.21	200.12	1.10	4.32E-03
	hsa-miR-1469	3,533.57	7,305.28	1.08	8.23E-12
	hsa-miR-2861	2,736.42	5,341.13	0.96	3.33E-16
	hsa-miR-4281	4,284.57	7,921.97	0.96	8.70E-07
	hsa-miR-1915	4,431.97	8,047.89	0.86	8.20E-14
	hsa-miR-3656	11,330.38	18,409.56	0.69	7.11E-15
	hsa-miR-638	13,600.24	19,788.46	0.58	8.01E-03
	hsa-miR-3196	11,054.43	15,807.10	0.55	9.72E-04
	hsa-miR-3665	31,401.19	40,456.65	0.42	2.90E-11
33 miRNAs downregulated					
	hsa-miR-451	344.64	16.49	-4.57	5.33E-15
	hsa-miR-486-5p	266.95	34.91	-3.06	6.98E-14
	hsa-miR-22	315.21	96.19	-1.71	1.68E-06
	hsa-miR-3613-3p	2,585.51	822.50	-1.70	2.99E-06
	hsa-miR-99a	328.12	114.31	-1.52	2.98E-06
	hsa-miR-19b	209.96	73.48	-1.49	6.49E-05
	hsa-miR-222	5,649.12	2,043.55	-1.47	4.94E-05
	hsa-miR-31	661.67	283.37	-1.19	4.33E-07
	hsa-miR-100	4,518.84	2,098.59	-1.10	5.55E-16
	hsa-miR-29a	5,529.50	2,599.13	-1.05	3.26E-06
	hsa-miR-125b	3,314.44	1,667.47	-0.99	1.78E-13
	hsa-miR-221	2,701.58	1,377.80	-0.98	1.11E-16
	hsa-miR-27a	1,538.29	818.39	-0.94	1.64E-09
	hsa-miR-17	1,736.28	944.55	-0.89	5.00E-10
	hsa-miR-24	3,914.53	2,113.81	-0.88	2.90E-12
	hsa-miR-16	3,982.38	2,191.03	-0.86	5.95E-14
	hsa-miR-1280	7,249.43	4,059.76	-0.84	1.55E-15
	hsa-miR-1260b	2,453.50	1,379.86	-0.82	3.69E-11
	hsa-miR-106a	1,585.07	913.50	-0.80	9.34E-08
	hsa-miR-30a	598.77	359.81	-0.72	2.84E-05
	hsa-miR-23b	11,820.23	7,363.01	-0.69	1.11E-16
	hsa-miR-23a	17,287.14	11,471.30	-0.64	8.22E-12
	hsa-miR-191	1,904.74	1,257.13	-0.63	1.92E-05
	hsa-miR-107	1,144.24	751.05	-0.62	7.16E-04
	hsa-miR-20a	1,855.18	1,222.77	-0.60	3.92E-07
	hsa-miR-103	1,356.94	934.27	-0.57	3.86E-05
	hsa-let-7a	11,124.80	7,747.60	-0.55	4.23E-13

Table III. Continued.

	microRNAs[a]	Non-SP signal[b]	SP signal[c]	$\log_2$ (SP signal/non-SP signal)[d]	P-value[e]
33 miRNAs downregulated					
	hsa-miR-92a	4,273.21	3076.71	-0.52	1.33E-12
	hsa-miR-320a	1,672.15	1,246.14	-0.43	5.09E-04
	hsa-let-7d	5,945.60	4,671.88	-0.35	6.94E-08
	hsa-miR-21	20,993.52	16,794.82	-0.31	1.12E-13
	hsa-let-7c	6,075.31	4,871.67	-0.30	1.10E-03
	hsa-let-7f	5,936.56	5,009.06	-0.29	6.21E-04

[a]A total of 1208 miRNAs were analyzed using miRNA microarray (LC Sciences). [b]Hybridization signal of miRNAs in non-SP. [c]Hybridization signal of miRNAs in SP. [d]Positive and negative $\log_2$ scores signify upregulation and downregulation, respectively. [e]miRNAs were analyzed as described in Materials and methods. The data are presented as P-value in SP compared with non-SP. Only P-values that were significantly (P<0.01) decreased or increased are shown. These values represent the mean of five biological replicates.

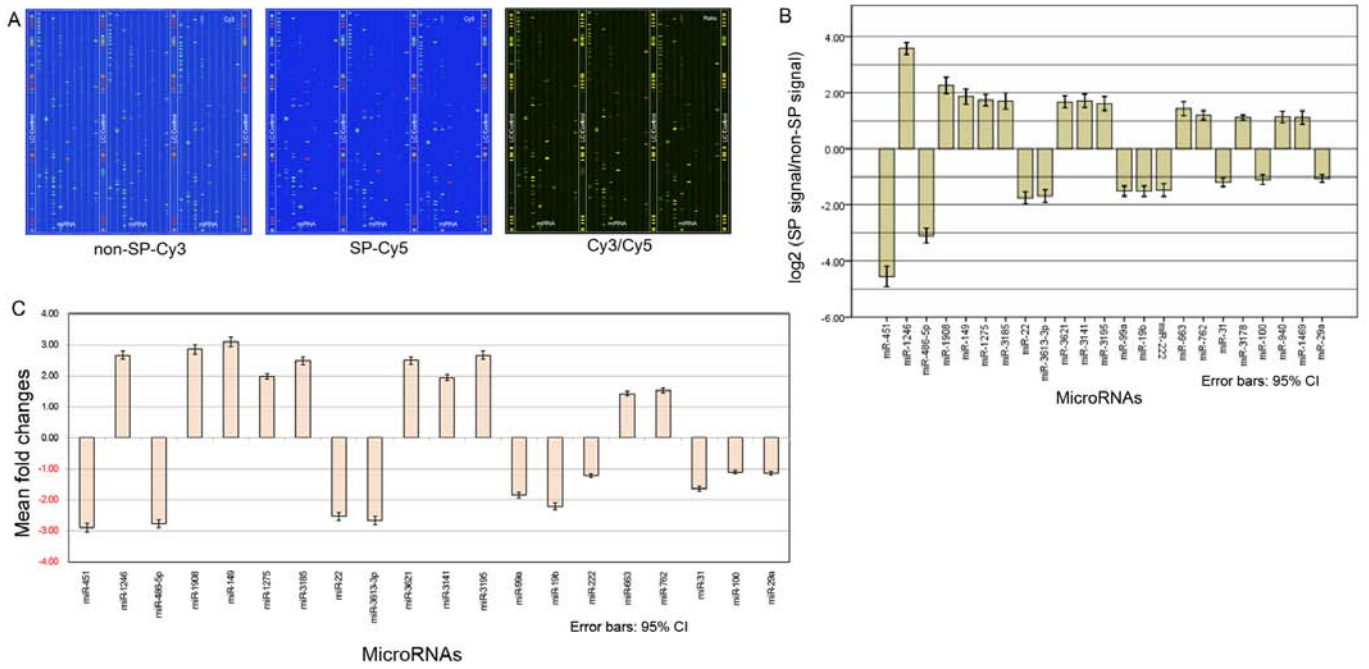

Figure 4. Expression profiling of miRNAs and qRT-PCR validation results. (A) An image of the miRNA biochip for the SP and non-SP groups, (B) a subset of the significantly differentially expressed miRNAs, and (C) the P-value and fold change of miRNAs for the comparison between the SP and non-SP groups by qRT-PCR validation. *P<0.05, **P<0.01.

than the negative control group; and there was no significant difference in the number of cells in the G2/M phase among the three groups. Fig. 5C depicts the results of the MTT assay. The OD value represents the degree of cell proliferation. A greater OD value indicates more cell proliferation. As shown in Fig. 5C, the proliferation rate of the micro down group was significantly lower than the other two groups. Fig. 5D shows the results of the apoptosis assay in which the number of apoptotic cells in the micro down group was significantly higher than the other two groups.

Downregulation of miRNA-149 leads to a significant reduction in the colony formation potential of TSU-derived SP cells. A classic colony formation assay was performed to analyze the potential change in colony formation potential for TSU-derived SP cells when miRNA-149 was downregulated. Fig. 6A shows the digital photos in which the colony formation cells were stained with Giemsa solution. The data analysis showed that the number of clones in the micro down group was significantly less than the other two groups (Fig. 6B). Fig. 6C depicts a representative cell morphology for a clone using either phase contrast or fluorescence microscopy and, finally, Giemsa staining. The clones formed from the micro down group contained fewer and more dispersed cells.

Downregulation of miRNA-149 in TSU-derived SP cells inhibits tumor growth in vivo. There were visible tumors in the control group and the NC group from the 7th day after

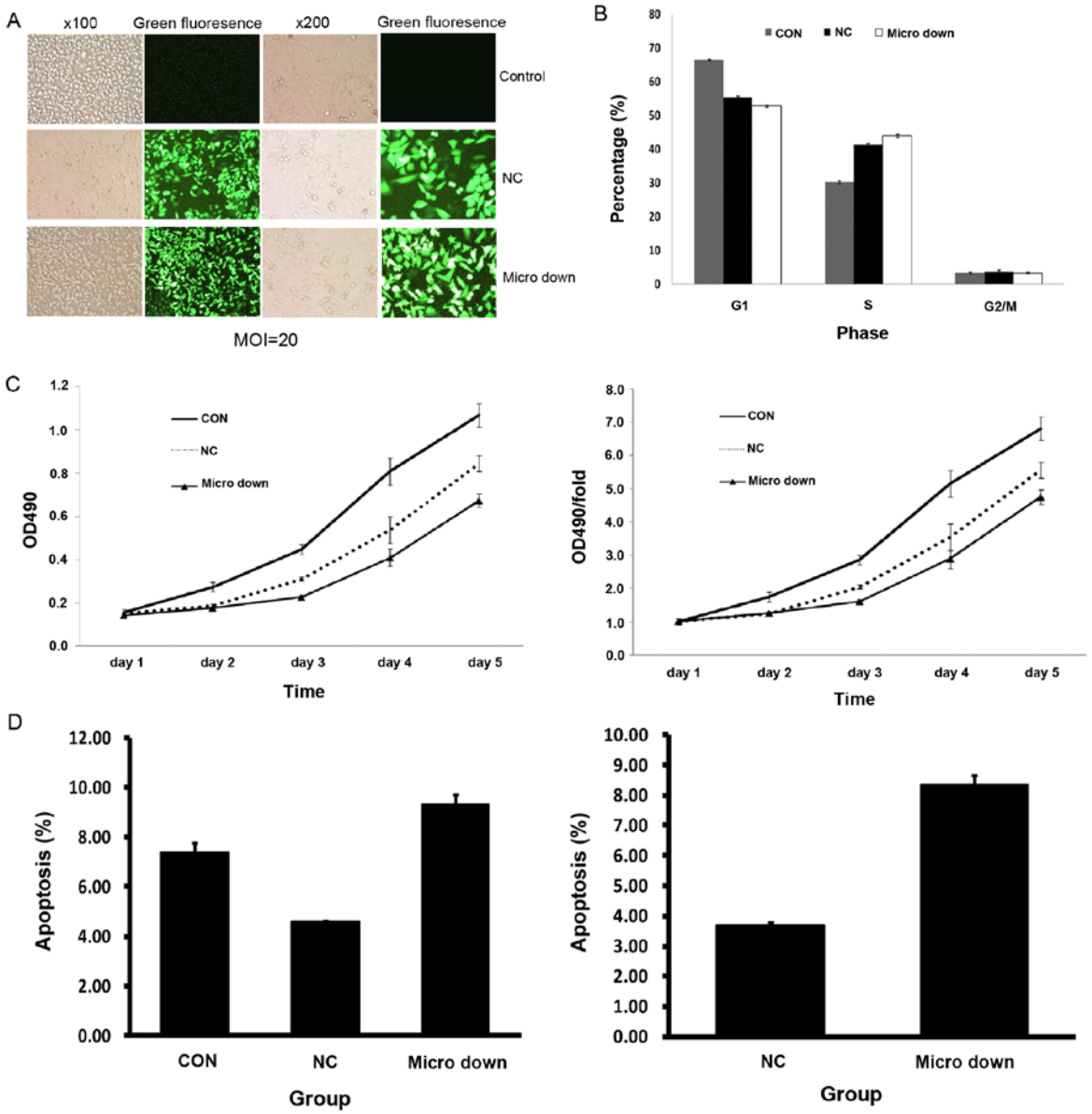

Figure 5. Cell proliferation and apoptosis. (A) Representative images of the three groups, which were treated under the same conditions including the same media, culture time, and MOI (MOI=20); (control) uninfected TSU-derived SP cells (negative control) TSU-derived SP cells infected with the empty lentiviral vector, (micro down) TSU-derived SP cells infected with the constructed lentivirus containing the miRNA-149-inhibition fragment. (B) The results of the cell cycle assay, (C) the MTT assay, (D) and apoptosis assay. *P<0.05, **P<0.01.

inoculation, whereas tumor growth was not observed in micro down group until the 13th day (Fig. 7). Until the 37th day before the end of the experiment, we observed tumors in 3 out of 4 mice from the control group, 2 out of 4 in the NC group (one mouse died of unknown causes on the 7th day) and 2 out of 4 in the micro down group (Fig. 7A). Images of the formed tumors are shown in Fig. 7B. The difference of tumorigenicity among the three groups is readily apparent. We also determined a tumor growth curve for each group and found that the mean growth rate of tumors in the micro down group was notably lower than the other two groups (Fig. 7C). Fig. 7D shows immunohistochemistry images for the three groups. H&E staining verified that all of the masses were tumors. Ki-67 indicates the distribution of the proliferating cells (dark brown staining), and Bax staining depicts an apoptotic protein in the cytoplasm and nucleus that is dyed brown. All of the above methods demonstrated that the downregulation of miRNA-149 in TSU-derived SP cells inhibits tumor growth *in vivo*.

Discussion

Because normal prostate and prostate cancer cells are susceptible to androgen regulation (35), early prostate cancer can be controlled using androgen suppression. However, most prostate cancer patients develop androgen-independent prostate cancer (AIPC), which is very difficult to treat (36). These clinical difficulties have forced us to change our ways of thinking to create fundamentally new avenues for the treatment of prostate cancer. Continuous progress in cancer research has provided accumulating evidence for the existence of a small group of cancer stem cells in many types of tumor tissues, which could be the cause of prostate cancer metastasis and recurrence as

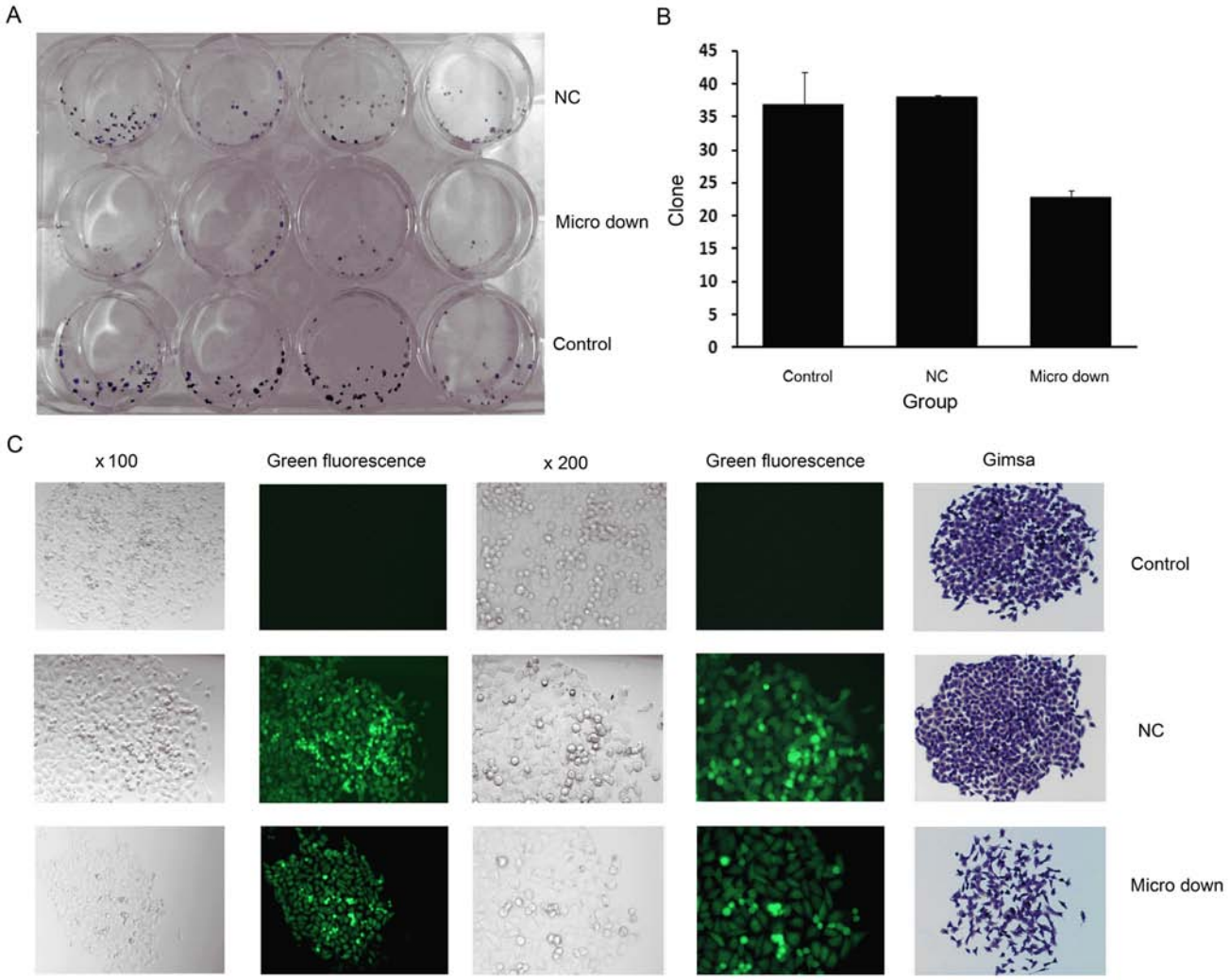

Figure 6. Colony formation experiment. (A) The digital photos of the formed colonies that were stained with Giemsa solution, (B) the data analysis of the number of clones in the three groups, and (C) the cell morphology of a representative clone in different backgrounds, including phase-contrast, fluorescence and bright field of the Giemsa staining. *P<0.05, **P<0.01.

well as hormone-dependent receptor changes. To some extent, prostate cancer is a stem cell disease. Prostate cancer stem cells (PCSC) have the same characteristics as stem cells, such as self-renewal, multi-differentiation, the capacity for unlimited proliferation, immortalized resistance and high tumor rates. More importantly, they are the tumor initiating cells and form tumor cell heterogeneity through abnormal differentiation. The identification of CSCs provides a new path for the exploration of mechanisms underlying tumor formation. Many studies have tried to transfer this new idea into tumor prognostic and predictive information (37). Through a tumor hierarchical pattern study, CSCs could originate from normal tissue stem cells that have existed for a long time (38). Therefore, the surface markers of normal tissue stem cells may also exist on the surface of homologous CSCs. For example, the stem cell surface marker CD44^{+} of colon cancer also exists in normal colon cells (39); the stem cell marker CD133^{+} of ovarian cancer (40), ALDH1^{+} of lung cancer (41), and the stem cell phenotype SP of endometrial cancer all also exist in the corresponding normal cells of these tissues (42). By looking for the same marker, tumor stem cells could potentially be isolated from tumor tissue. However, specific stem cell surface markers for many tumor tissues are still undefined, thus, it remains difficult to use a certain type of stem cell surface marker to select and identify prostate cancer stem cells. Recent studies have found that SP cells not only exist in the hematopoietic system, but are also distributed in a variety of normal tissues, tumor cell lines and solid tumors, including almost all normal human tissues such as blood, the liver, lungs, skin, breasts and ovarian cancer, nasopharyngeal carcinoma, and tumors of the nervous system (43,44). Moreover, from the investigation of many types of tumor cell lines and tumor tissues, SP cells have been found to have the biological characteristics of self-renewal, multipotent differentiation, a slow cell cycle, high-tumorigenic force, and tolerance to radioactive substances and chemotherapy drugs, which are similar to the biological characteristics of CSCs. The discovery of an SP subgroup is very practical for solid tumor stem cell research, especially when specific cell surface markers have not been found. Therefore, it can be used as an effective method for stem cell research. In the early stages, we used a side population cell flow sorting method to separate and culture SP cells from the prostate cancer cell lines LNCaP PC-3, TSU and DU145, which are common cultured cell lines. Using a wide

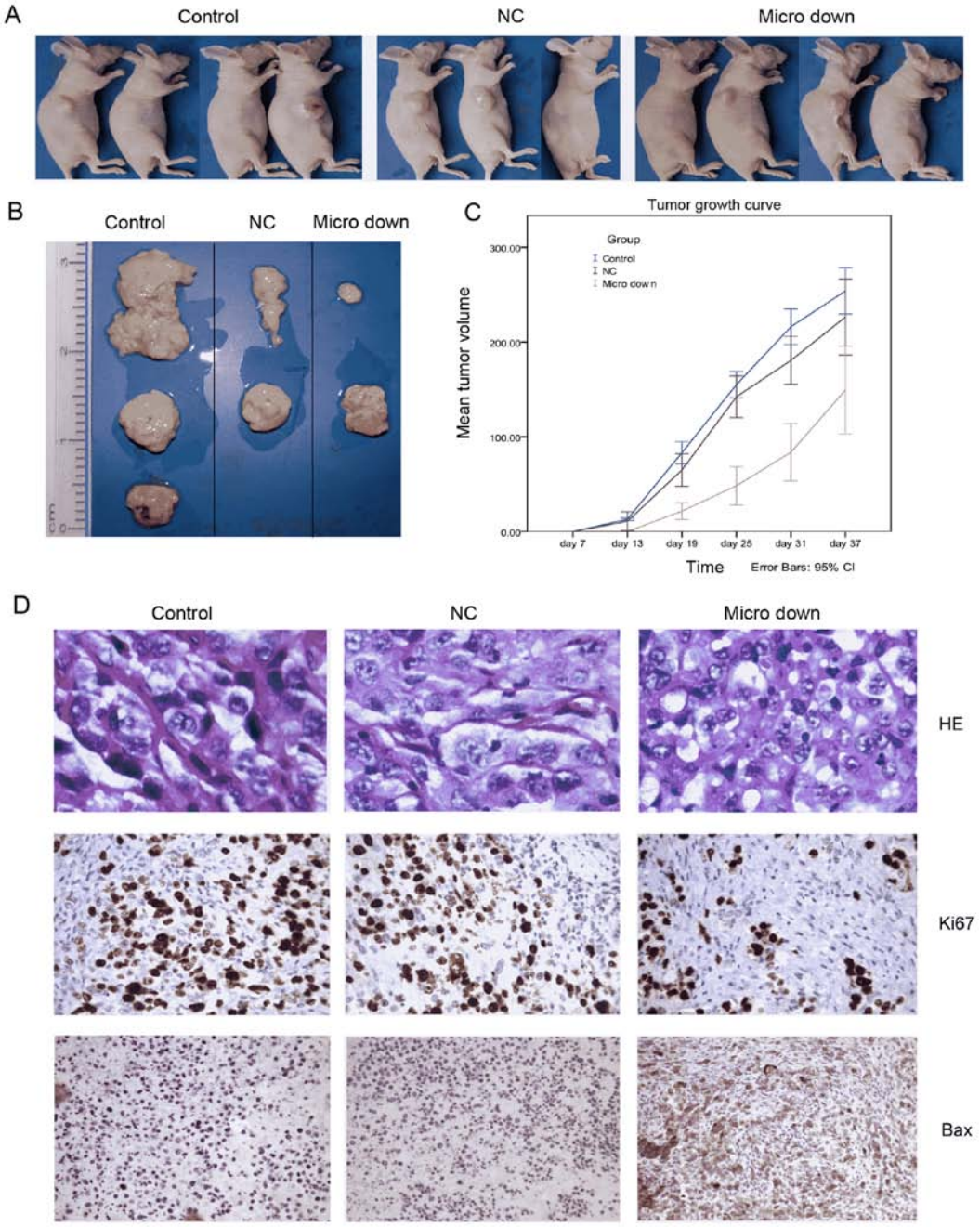

Figure 7. Tumor growth *in vivo*. (A) The images of mice 37 days after injecting the same number of cells from the three different groups, (B) images of the formed tumors, (C) the tumor growth curve of the three different groups, and (D) immunohistochemistry images for H&E staining, Ki-67 staining, and Bax staining in the three groups. *P<0.05, **P<0.01.

methodological range of experiments to identify the characteristics of CSCs from SP cells, it was found that side population cells are prevalent in common prostate cancer. According to the different types of prostate cancer cell lines, the proportion of SP cells ranges from 0.6 to 1.6%. SP cells have the characteristics of high CSC proliferation and tumorigenesis (45).

Cancer stem cells and miRNAs have become hot issues in the oncology research community in recent years. If effectively combined, they will be helpful in explaining the molecular mechanisms underlying the biological characteristics of CSCs, and could create new ways for cancer treatment and prognosis. The present study mainly focuses on the expression and functional differences of miRNAs between ordinary tumor cells and normal tissue cells from the same source, so as to infer the occurrence and biological characteristics of the tumor. However, the comparative studies on CSCs, the source of tumors, have been less effective. miRNAs may become a promising new anti-angiogenic target for cancer (46,47). For example, hsa-miR-149 is the earliest discovered human small molecule RNA. A recent study found that hsa-miR-149 plays a regulatory role in the occurrence of gastric cancer. miRNAs may serve as potential biomarkers and therapeutic targets for gastric cancer (48). A number of studies have used large sample statistics and gene expression analysis to show that habits such as smoking and tea-drinking can cause changes in the regulation of hsa-miR-149 and increase one's susceptibility to gastric

cancer (49). We have used advanced flow sorting, biochip and real-time quantitative PCR detection technology to effectively select tumor cells and then to explore the changes in CSCs and ordinary tumor cells at the molecular level, mainly in miRNA expression and functional regulation, to discover the origin and fundamental mechanisms underlying tumorigenesis. However, our experiments also have some limitations. If we could add normal tissue cells from the same source to compare and analyze the changes in miRNAs found in CSCs, ordinary tumor cells and normal tissue cells, our results would be more persuasive.

The miRNA biochip experiment is the key and core of the present study. To ensure the smooth process of the experiment and the accuracy and reliability of the results, sample preparation is particularly important. To provide 2-3 μg of total RNA (the small RNA amount is >0.5 μg), the steps of cell culture and flow sorting should be strictly controlled to ensure obtaining $>10^6$ cells with good cell activity. When performing the total RNA extraction, an important step is to ensure that the small RNA are retained during the process. Compared with a column method, an RNA extraction kit can better ensure the purity of the small RNA. For transportation, the sample is relatively stable in the form of total RNA. qRT-PCR experiments can further verify specifically selected miRNA and improve the accuracy of the experiment. We adopted a probe method for the qRT-PCR experiment because its specificity and accuracy are higher than the fluorescent dye method and more suitable for small RNA research. A miRNA expression interference experiment is the most common method to study the function of miRNAs in cells (50). miRNA mimics or inhibitors constructed by lentiviral vectors can efficiently infect the target cells to promote or inhibit the corresponding miRNA expression in these cells and study their function. This method has been widely used by researchers (51-53). For example, lentivirus-mediated interference to knock down eukaryotic translation initiation factor 3 subunit D expression inhibits proliferation of HCT116 colon cancer cells (54). Downregulation of β2SP by lentivirus short hairpin RNA activates Notch signaling and SOX9 expression in esophageal adenocarcinoma (55). We used a constructed miRNA-149-inhibition lentivirus to infect SP cells from the TSU cell line and explored the best conditions for infection, which laid the foundation for our subsequent experiments. Cell function experiments confirmed that the downregulation of miRNA-149 expression could significantly decrease the *in vitro* proliferation and colony formation capacity of TSU-derived SP cells, promote apoptosis and inhibit the growth rate of tumors. This may be related to miRNA-149's activation of intracellular signal transduction pathways (56), an idea that further specific experiments can confirm.

Although the research on CSCs has rapidly progressed over the past few years, there are still many critical issues that need to be resolved. The present study not only establishes a technical platform for human prostate cancer stem cell sorting, but more importantly, it provides a basis for the study of miRNA's biological functions in human prostate cancer stem cells. The research and application of CSCs and miRNAs are still in their initial stages, and many problems such as developmental status, biological properties, related function and their relationship with tumor occurrence need reasonable and complete theories. Therefore, deeper study and exploration of CSCs and miRNA regulation relationships are necessary. It is believed that with the progress of research technology and the advanced research on CSCs by domestic and foreign counterparts, the identification of specific markers and related signal transduction pathways of CSCs will be discovered, which will have practical significance for the early prevention, diagnosis, efficient drug therapy, recurrence and metastasis and prognosis of cancers.

Acknowledgements

The present study was supported by the National Natural Science Foundation of China (no. 81341066) and the Special Foundation for High Level of Health Personnel of Beijing Health System (no. 2013-2-003).

References

1. Li S and Li Q: Cancer stem cells and tumor metastasis (Review). Int J Oncol 44: 1806-1812, 2014.
2. Routray S and Mohanty N: Cancer stem cells accountability in progression of head and neck squamous cell carcinoma: The most recent trends! Mol Biol Int 2014: 375325, 2014.
3. Wang D, Zhu H, Liu Y, Liu Q, Xie X, Zhou Y, Zhang L, Zhu Y, Zhang Z and Su Z: The low chamber pancreatic cancer cells had stem-like characteristics in modified transwell system: Is it a novel method to identify and enrich cancer stem-like cells? BioMed Res Int 2014: 760303, 2014.
4. Wang J, Ma Y and Cooper MK: Cancer stem cells in glioma: Challenges and opportunities. Transl Cancer Res 2: 429-441, 2013.
5. Wieczorek K and Niewiarowska J: Cancer stem cells. Postepy Hig Med Dosw Online 66: 629-636, 2012 (In Polish).
6. Qi W, Zhao C, Zhao L, Liu N, Li X, Yu W and Wei L: Sorting and identification of side population cells in the human cervical cancer cell line HeLa. Cancer Cell Int 14: 3, 2014.
7. Wouters J, Stas M, Gremeaux L, Govaere O, Van den Broeck A, Maes H, Agostinis P, Roskams T, van den Oord JJ and Vankelecom H: The human melanoma side population displays molecular and functional characteristics of enriched chemoresistance and tumorigenesis. PLoS One 8: e76550, 2013.
8. Mendell JT and Olson EN: MicroRNAs in stress signaling and human disease. Cell 148: 1172-1187, 2012.
9. Tessitore A, Cicciarelli G, Del Vecchio F, Gaggiano A, Verzella D, Fischietti M, Vecchiotti D, Capece D, Zazzeroni F and Alesse E: MicroRNAs in the DNA damage/repair network and cancer. Int J Genomics 2014: 820248, 2014.
10. Cadamuro AC, Rossi AF, Maniezzo NM and Silva AE: *Helicobacter pylori* infection: Host immune response, implications on gene expression and microRNAs. World J Gastroenterol 20: 1424-1437, 2014.
11. Litvinov IV and Peh K: Connecting the dots in cutaneous T cell lymphoma (CTCL): STAT5 regulates malignant T cell proliferation via miR-155. Cell Cycle 12: 1939-1947, 2013.
12. Undi RB, Kandi R and Gutti RK: MicroRNAs as haematopoiesis regulators. Adv Hematol 2013: 695754, 2013.
13. Lawson SK, Dobrikova EY, Shveygert M and Gromeier M: p38α mitogen-activated protein kinase depletion and repression of signal transduction to translation machinery by miR-124 and -128 in neurons. Mol Cell Biol 33: 127-135, 2013.
14. Adlakha YK and Saini N: Brain microRNAs and insights into biological functions and therapeutic potential of brain enriched miRNA-128. Mol Cancer 13: 33, 2014.
15. Nagpal N and RituKulshreshtha: miR-191: an emerging player in disease biology. Front Genet 5: 1-10, 2014.
16. Li M, Guan X, Sun Y, Mi J, Shu X, Liu F and Li C: miR-92a family and their target genes in tumorigenesis and metastasis. Exp Cell Res 323: 1-6, 2014.
17. Qin Q, Furong W and Baosheng L: Multiple functions of hypoxia-regulated miR-210 in cancer. J Exp Clin Cancer Res 33: 50, 2014.

18. Konno Y, Dong P, Xiong Y, Suzuki F, Lu J, Cai M, Watari H, Mitamura T, Hosaka M, Hanley SJ, *et al*: MicroRNA-101 targets EZH2, MCL-1 and FOS to suppress proliferation, invasion and stem cell-like phenotype of aggressive endometrial cancer cells. Oncotarget 5: 6049-6062, 2014.
19. Wu K, Yang L, Li C, Zhu CH, Wang X, Yao Y and Jia YJ: MicroRNA-146a enhances *Helicobacter pylori* induced cell apoptosis in human gastric cancer epithelial cells. Asian Pac J Cancer Prev 15: 5583-5586, 2014.
20. Peng Y, Liu YM, Li LC, Wang LL and Wu XL: MicroRNA-338 inhibits growth, invasion and metastasis of gastric cancer by targeting NRP1 expression. PloS one 9: e94422, 2014.
21. Zhu ED, Li N, Li BS, Li W, Zhang WJ, Mao XH, Guo G, Zou QM and Xiao B: miR-30b, down-regulated in gastric cancer, promotes apoptosis and suppresses tumor growth by targeting plasminogen activator inhibitor-1. PLoS One 9: e106049, 2014.
22. Zhang F, Yang Z, Cao M, Xu Y, Li J, Chen X, Gao Z, Xin J, Zhou S, Zhou Z, *et al*: MiR-203 suppresses tumor growth and invasion and down-regulates MiR-21 expression through repressing Ran in esophageal cancer. Cancer Lett 342: 121-129, 2014.
23. Zhang ZC, Li YY, Wang HY, Fu S, Wang XP, Zeng MS, Zeng YX and Shao JY: Knockdown of miR-214 promotes apoptosis and inhibits cell proliferation in nasopharyngeal carcinoma. PLoS One 9: e86149, 2014.
24. Zhao Y, Miao G, Li Y, Isaji T, Gu J, Li J and Qi R: MicroRNA-130b suppresses migration and invasion of colorectal cancer cells through downregulation of integrin β1 [corrected]. PLoS One 9: e87938, 2014.
25. Bao Y, Chen Z, Guo Y, Feng Y, Li Z, Han W, Wang J, Zhao W, Jiao Y and Li K: Tumor suppressor microRNA-27a in colorectal carcinogenesis and progression by targeting SGPP1 and Smad2. PLoS One 9: e105991, 2014.
26. Du B, Wang Z, Zhang X, Feng S, Wang G, He J and Zhang B: MicroRNA-545 suppresses cell proliferation by targeting cyclin D1 and CDK4 in lung cancer cells. PLoS One 9: e88022, 2014.
27. Wang N, Liang H, Zhou Y, Wang C, Zhang S, Pan Y, Wang Y, Yan X, Zhang J and Zhang CY: miR-203 suppresses the proliferation and migration and promotes the apoptosis of lung cancer cells by targeting SRC. PLoS One 9: e105570, 2014.
28. Ip J, Canham P, Choo KH, Inaba Y, Jacobs SA, Kalitsis P, Mattiske DM, Ng J, Saffery R, Wong NC, *et al*: Normal DNA methylation dynamics in DICER1-deficient mouse embryonic stem cells. PLoS Genet 8: e1002919, 2012.
29. Rosa A and Brivanlou AH: Regulatory non-coding RNAs in pluripotent stem cells. Int J Mol Sci 14: 14346-14373, 2013.
30. Bier A, Giladi N, Kronfeld N, Lee HK, Cazacu S, Finniss S, Xiang C, Poisson L, deCarvalho AC, Slavin S, *et al*: MicroRNA-137 is downregulated in glioblastoma and inhibits the stemness of glioma stem cells by targeting RTVP-1. Oncotarget 4: 665-676, 2013.
31. Floyd DH, Zhang Y, Dey BK, Kefas B, Breit H, Marks K, Dutta A, Herold-Mende C, Synowitz M and Glass R: Novel anti-apoptotic microRNAs 582-5p and 363 promote human glioblastoma stem cell survival via direct inhibition of caspase-3, caspase-9, and Bim. PLoS One 9: e96239, 2014.
32. Li R, Zhang L, Jia L, Duan Y, Li Y, Wang J, Bao L and Sha N: MicroRNA-143 targets Syndecan-1 to repress cell growth in melanoma. PLoS One 9: e94855, 2014.
33. Wallace TJ, Torre T, Grob M, Yu J, Avital I, Brücher B, Stojadinovic A and Man YG: Current approaches, challenges and future directions for monitoring treatment response in prostate cancer. J Cancer 5: 3-24, 2014.
34. Chen Y, Zhao J, Luo Y, Wang Y, Wei N and Jiang Y: Isolation and identification of cancer stem-like cells from side population of human prostate cancer cells. J Huazhong Univ Sci Technolog Med Sci 32: 697-703, 2012.
35. Pelekanou V, Notas G, Stathopoulos EN, Castanas E and Kampa M: Androgen receptors in early and castration resistant prostate cancer: Friend or foe? Hormones (Athens) 12: 224-235, 2013.
36. Saraon P, Jarvi K and Diamandis EP: Molecular alterations during progression of prostate cancer to androgen independence. Clin Chem 57: 1366-1375, 2011.
37. Maugeri-Saccà M and Maria RD: Translating basic research in cancer patient care. Ann Ist Super Sanita 47: 64-71 2011.
38. Bussolati B, Grange C and Camussi G: Tumor exploits alternative strategies to achieve vascularization. FASEB J 25: 2874-2882, 2011.
39. Sanders MA and Majumdar APN: Colon cancer stem cells: Implications in carcinogenesis. Front Biosci (Landmark Ed) 16: 1651-1662, 2011.
40. Silva IA, Bai S, McLean K, Yang K, Griffith K, Thomas D, Ginestier C, Johnston C, Kueck A, Reynolds RK, *et al*: Aldehyde dehydrogenase in combination with CD133 defines angiogenic ovarian cancer stem cells that portend poor patient survival. Cancer Res 71: 3991-4001, 2011.
41. Jiang F, Qiu Q, Khanna A, Todd NW, Deepak J, Xing L, Wang H, Liu Z, Su Y, Stass SA, *et al*: Aldehyde dehydrogenase 1 is a tumor stem cell-associated marker in lung cancer. Mol Cancer Res 7: 330-338, 2009.
42. Kato K, Kuhara A, Yoneda T, Inoue T, Takao T, Ohgami T, Dan L, Kuboyama A, Kusunoki S, Takeda S, *et al*: Sodium butyrate inhibits the self-renewal capacity of endometrial tumor side-population cells by inducing a DNA damage response. Mol Cancer Ther 10: 1430-1439, 2011.
43. Kong QL, Hu LJ, Cao JY, Huang YJ, Xu LH, Liang Y, Xiong D, Guan S, Guo BH, Mai HQ, *et al*: Epstein-Barr virus-encoded LMP2A induces an epithelial-mesenchymal transition and increases the number of side population stem-like cancer cells in nasopharyngeal carcinoma. PLoS Pathog 6: e1000940, 2010.
44. Harris MA, Yang H, Low BE, Mukherjee J, Guha A, Bronson RT, Shultz LD, Israel MA and Yun K: Cancer stem cells are enriched in the side population cells in a mouse model of glioma. Cancer Res 68: 10051-10059, 2008.
45. Richard V, Nair MG, Santhosh Kumar TR and Pillai MR: Side population cells as prototype of chemoresistant, tumor-initiating cells. BioMed Res Int 2013: 517237, 2013.
46. Gallach S, Calabuig-Fariñas S, Jantus-Lewintre E and Camps C: MicroRNAs: promising new antiangiogenic targets in cancer. Biomed Res Int 2014: 878450, 2014.
47. Di Leva G, Garofalo M and Croce CM: MicroRNAs in cancer. Annu Rev Pathol 9: 287-314, 2014.
48. Shin VY and Chu KM: MiRNA as potential biomarkers and therapeutic targets for gastric cancer. World J Gastroenterol 20: 10432-10439, 2014.
49. Wang Y, Zheng X, Zhang Z, Zhou J, Zhao G, Yang J, Xia L, Wang R, Cai X, Hu H, *et al*: MicroRNA-149 inhibits proliferation and cell cycle progression through the targeting of ZBTB2 in human gastric cancer. PLoS One 7: e41693, 2012.
50. Franceschini A, Meier R, Casanova A, Kreibich S, Daga N, Andritschke D, Dilling S, Rämö P, Emmenlauer M, Kaufmann A, *et al*: Specific inhibition of diverse pathogens in human cells by synthetic microRNA-like oligonucleotides inferred from RNAi screens. Proc Natl Acad Sci USA 111: 4548-4553, 2014.
51. Shin B, Oh H, Park SM, Han HE, Ye M, Song WK and Park WJ: Intracellular cleavage of amyloid β by a viral protease NIa prevents amyloid β-mediated cytotoxicity. PLoS One 9: e98650, 2014.
52. Grandchamp N, Altémir D, Philippe S, Ursulet S, Pilet H, Serre MC, Lenain A, Serguera C, Mallet J and Sarkis C: Hybrid lentivirus-phiC31-int-NLS vector allows site-specific recombination in murine and human cells but induces DNA damage. PLoS One 9: e99649, 2014.
53. Chu SC, Hsieh YS, Yu CC, Lai YY and Chen PN: Thymoquinone induces cell death in human squamous carcinoma cells via caspase activation-dependent apoptosis and LC3-II activation-dependent autophagy. PLoS One 9: e101579, 2014.
54. Yu X, Zheng B and Chai R: Lentivirus-mediated knockdown of eukaryotic translation initiation factor 3 subunit D inhibits proliferation of HCT116 colon cancer cells. Biosci Rep 5: 1-17, 2014.
55. Song S, Maru DM, Ajani JA, Chan CH, Honjo S, Lin HK, Correa A, Hofstetter WL, Davila M, Stroehlein J, *et al*: Loss of TGF-β adaptor β2SP activates notch signaling and SOX9 expression in esophageal adenocarcinoma. Cancer Res 73: 2159-2169, 2013.
56. Pei N, Jie F, Luo J, Wan R, Zhang Y, Chen X, Liang Z, Du H, Li A, Chen B, *et al*: Gene expression profiling associated with angiotensin II type 2 receptor-induced apoptosis in human prostate cancer cells. PLoS One 9: e92253, 2014.